A&A 499, 661–667 (2009)
DOI: 10.1051/0004-6361/200811272

Astronomy & Astrophysics

Analytic fitting formulae for relativistic electron-electron thermal bremsstrahlung

S. Nozawa[1], K. Takahashi[2], Y. Kohyama[2], and N. Itoh[2]

[1] Josai Junior College, 1-1 Keyakidai, Sakado-shi, Saitama, 350-0295, Japan
e-mail: snozawa@josai.ac.jp
[2] Department of Physics, Sophia University, 7-1 Kioi-cho, Chiyoda-ku, Tokyo, 102-8554, Japan
e-mail: n_itoh@sophia.ac.jp

Received 1 November 2008 / Accepted 18 February 2009

ABSTRACT

We present accurate analytic fitting formulae for electron-electron thermal bremsstrahlung emissivity. The fitting formulae have an overall accuracy of higher than 0.5% for a wide electron temperature range 1 keV $\leq k_{\rm B}T \leq$ 7 MeV, which will be useful when analyzing the precision observational data from the non-relativistic regime to mildly-relativistic regime. Assuming the thermal plasma, the present formulae will be also applicable to the relativistic regime.

Key words. cosmology: theory – galaxies: clusters: general – radiation mechanisms: thermal – relativity – X-rays: galaxies: clusters

1. Introduction

Following the launch of the *Chandra X-Ray Observatory*, the *XMM-Newton Observatory*, and the *Suzaku X-ray Observatory*, X-ray astronomy has entered its own era of precision science. In particular, these satellites have revolutionized the accuracy of the observational data available for galaxy clusters (for example, Allen et al. 2001; Schmidt et al. 2001; Sato et al. 2007). The precision observational data taken by these satellites require precision basic physics data for their analysis.

The present authors have published a series of papers in which they have completed accurate calculations for the electron-ion thermal bremsstrahlung process. These are particularly suited to the analysis of radiation process in high-temperature galaxy clusters (Nozawa et al. 1998; Itoh et al. 2000, 2002b). In Itoh et al. (2000, 2002b), the present authors presented accurate analytic fitting formulae for the electron-ion thermal bremsstrahlung Gaunt factors, which have a general accuracy of about 0.1% for the ranges $1 \leq Z_j \leq 28$, $6.0 \leq \log T[\mathrm{K}] \leq 8.5$, where Z_j is the charge of the ion and T is the electron temperature. These electron-ion thermal bremsstrahlung Gaunt factors are also suitable for the analysis of the precision X-ray data of galaxy clusters taken by the *Chandra*, the *XMM-Newton* and the *Suzaku Observatories*.

It has been known for some time that the electron-electron thermal bremsstrahlung makes a percent-order contribution to the thermal bremsstrahlung at low temperature $T \sim 10^8$ K (Maxon & Corman 1967; Maxon 1972; Haug 1975a,b; Svensson 1982; Dermer 1986). In particular, Haug (1975a) and Haug (1975b) carried out a relativistic calculation of the electron-electron thermal bremsstrahlung emissivity and found that the non-relativistic electron-electron thermal bremsstrahlung emissivity calculated Maxon & Corman (1967) and Maxon (1972) agree with the relativistic results to within about 1% accuracy at $T \sim 1.5 \times 10^8$ K. Itoh et al. (2002a) calculated the precision analytic fitting formula for the non-relativistic electron-electron thermal bremsstrahlung Gaunt factor, which has an overall accuracy of higher than 1% for the temperature range $6.0 \leq \log\ T[\mathrm{K}] \leq 8.5$.

On the other hand, it is known that the electron-electron bremsstrahlung dominates the electron-ion bremsstrahlung for high energy electrons. In active galactic nuclei, gamma-ray bursters and compact binary sources, the electron energies may be greater than 100 keV. Stepney & Guilbert (1983) studied several important processes contributing to the high-temperature thermal plasmas. Among other processes, they presented analytic fitting formulae for the electron-electron thermal bremsstrahlung emissivity in the temperature range 50 keV $\leq k_{\rm B}T \leq$ 1 MeV. Their method was based upon the relativistic numerical calculation by Haug (1975a,b). Their fitting formulae have an overall accuracy that is higher than 5% compared with the numerical calculation by Haug (1975b).

In this paper, we present accurate analytic fitting formulae for the electron-electron thermal bremsstrahlung emissivity. The fitting formulae have an overall accuracy of higher than 0.5% for a wider electron temperature range 1 keV $\leq k_{\rm B}T \leq$ 7 MeV. The fitting formulae is suitable for the analysis of the precision observational data for electron energies from non-relativistic regime to mildly-relativistic regime. Assuming the thermal plasma, the present formulae will be also applicable to the relativistic regime. However, it should be remarked that the usefulness of the present formula is limited to relativistic plasma since we do not include the positron contribution. The photon production rate is dominated by $\mathrm{e}^+\mathrm{e}^-$ annihilations for the electron-positron pair equilibrium plasmas. Therefore, more careful study including the pair annihilation process will be necessary for the analysis of relativistic plasmas. The present paper is organized as follows. In Sect. 2, we will calculate the relativistic electron-electron thermal bremsstrahlung emissivity. In Sect. 3, we will present the precision analytic fitting formulae for the emissivity. Concluding remarks will be given in Sect. 4.

2. Electron-electron thermal bremsstrahlung

The expression for the thermally averaged relativistic electron-electron bremsstrahlung cross-section was derived by Haug (1975a, b). In this paper, we follow the notation used in Haug (1975a) unless otherwise noted. The number of photons emitted per unit time, per unit volume, and per unit energy interval by electron gas of uniform number density n_e at temperature T is given by Eq. (2.1) in Haug (1975b) and also by Eq. (A.1) in Stepney & Guilbert (1983) as follows:

$$\begin{aligned} P_{ee}(k,\tau) &= \frac{dN_{ee}}{dVdtdk} \\ &= \frac{cn_e^2}{[2\tau K_2(1/\tau)]^2}\int d\epsilon_1 e^{-\epsilon_1/\tau}\int d\epsilon_2 e^{-\epsilon_2/\tau} \\ &\quad\times\int d\mu\sqrt{\mu^2-1}\,\frac{d\sigma}{dk}, \end{aligned} \tag{1}$$

$$\begin{aligned} \frac{d\sigma}{dk} &= \frac{3}{8\pi^2}\alpha\sigma_T\int d\Omega_k\frac{k}{\omega\rho}\sqrt{\frac{\rho^2-4}{\omega^2-4}}\,f_{ee} \\ &\quad\times\frac{1}{\pi}\int A d\Omega_{p_1'}, \end{aligned} \tag{2}$$

where $k = h\nu/m_ec^2$ is the photon energy in units of the electron rest mass, $\tau = k_BT/m_ec^2$, $K_2(1/\tau)$ is the modified Bessel function of the second kind, α is the fine structure constant, and σ_T is the Thomson cross section, respectively. In Eq. (2) $\omega^2 = (p_1+p_2)^2$, $\rho^2 = (p_1'+p_2')^2$ and $\mu = p_1\cdot p_2$, where p_1 (p_1') and p_2 (p_2') are four momenta in units of the electron rest mass for the initial (final) electrons. We call $P_{ee}(k,\tau)$ the photon production rate for brevity. The explicit expression for $1/\pi\int A d\Omega_{p'}$ is given by appendix in Haug (1975a). In Eq. (2), f_{ee} is the Elwert factor, which takes into account the Coulomb corrections between two electrons (Elwert 1939). The explicit form is

$$f_{ee} = \frac{\beta_{12}}{\beta_{12}'}\frac{e^{2\pi\alpha/\beta_{12}}-1}{e^{2\pi\alpha/\beta_{12}'}-1}, \tag{3}$$

$$\beta_{12} = \frac{\omega\sqrt{\omega^2-4}}{\omega^2-2}, \tag{4}$$

$$\beta_{12}' = \frac{\rho\sqrt{\rho^2-4}}{\rho^2-2}. \tag{5}$$

It is known that the Coulomb corrections are important at low energies, whereas they are negligible for high energies.

Following Stepney & Guilbert (1983), where the z-axis is chosen to be parallel to the sum of the initial electron momenta, we rewrite Eq. (1) as follows:

$$P_{ee}(k,\tau) = n_e^2\sigma_Tc\alpha\frac{e^{-x}}{x}\frac{1}{\sqrt{\tau}}G(x,\tau), \tag{6}$$

where $x = k/\tau$ and $G(x,\tau)$ is defined by

$$\begin{aligned} G(x,\tau) &= \frac{3}{16\pi^2}\frac{x^2\sqrt{\tau}}{[2\exp(1/\tau)K_2(1/\tau)]^2}\int_0^\infty ds e^{-s} \\ &\quad\times\int_{-T_1}^{T_1}dt\int_{\mu_1}^{\mu_2}d\mu\int_0^{\theta_{max}}\frac{\sin\theta d\theta}{\sqrt{2(\mu+1-x)}} \\ &\quad\times\int_0^\pi d\phi f_{ee}\Sigma, \end{aligned} \tag{7}$$

$$\Sigma = \frac{\sqrt{\rho^2-4}}{\pi}\int A d\Omega_{p_1'}, \tag{8}$$

where θ is the zenith angle of photon. The boundary values of T_1, μ_1, μ_2 and θ_{max} are given in Appendix of Stepney & Guilbert (1983). Here it should be also noted that our definition of $G(x,\tau)$ in Eq. (6) differs from that of Eq. (4) in Stepney & Guilbert (1983) by a factor $\sqrt{\tau}$. Namely,

$$G_{SG}(x,\tau) = \frac{1}{\sqrt{\tau}}G(x,\tau), \tag{9}$$

where SG denotes Stepney & Guilbert.

Similarly, the total energy emitted per unit time, per unit volume (we refer to this as the emissivity for short) is given by

$$W_{ee}(\tau) = \frac{dE_{ee}}{dVdt} = m_ec^2\int_0^\infty dk k P_{ee}(k,\tau), \tag{10}$$

$$= m_ec^2n_e^2\sigma_Tc\alpha\tau^{3/2}G(\tau), \tag{11}$$

$$G(\tau) = \int_0^\infty dx e^{-x}G(x,\tau). \tag{12}$$

Equations (6)–(12) are our basic equations in the present paper. We performed the five-dimensional integration of Eq. (7) in the following range of 1 keV $\le k_BT \le$ 7 MeV for the electron temperature, and $10^{-4} \le x \le 10$ for the photon energy in units of the electron temperature.

It is known that the non-relativistic approximation is reliable at low temperatures, whereas the extreme-relativistic approximation is accurate at high temperatures. Here we study the extent of the approximations for the photon production rate and the emissivity. To ensure that the present paper is self-contained, we recall the expressions in these approximations. The photon production rate and the emissivity in the non-relativistic (NR) approximation (Maxon & Corman 1967; Maxon 1972; Itoh et al. 2002a) are given by

$$P_{ee}^{NR}(k,\tau) = n_e^2\sigma_Tc\alpha\frac{e^{-x}}{x}\frac{1}{\sqrt{\tau}}G^{NR}(x,\tau), \tag{13}$$

$$G^{NR}(x,\tau) = \frac{1}{5\pi^{3/2}}\int_0^\infty ds e^{-s}f_{ee}^{NR}A(x,s), \tag{14}$$

$$f_{ee}^{NR} = \sqrt{\frac{s+x}{s}}\frac{\exp\left(\frac{\pi\alpha}{\sqrt{\tau}}\frac{1}{\sqrt{s+x}}\right)-1}{\exp\left(\frac{\pi\alpha}{\sqrt{\tau}}\frac{1}{\sqrt{s}}\right)-1}, \tag{15}$$

$$\begin{aligned} A(x,s) &= \left\{17-3\left(\frac{x}{2s+x}\right)^2\right\}\sqrt{s(s+x)} \\ &\quad+(2s+x)\left\{12-7\left(\frac{x}{2s+x}\right)^2\right. \\ &\quad\left.-3\left(\frac{x}{2s+x}\right)^4\right\}\ln\frac{\sqrt{s}+\sqrt{s+x}}{\sqrt{x}}, \end{aligned} \tag{16}$$

$$W_{ee}^{NR}(\tau) = m_ec^2n_e^2\sigma_Tc\alpha\tau^{3/2}G^{NR}(\tau), \tag{17}$$

$$G^{NR}(\tau) = \int_0^\infty dx e^{-x}G^{NR}(x,\tau). \tag{18}$$

In Eq. (14) the Coulomb corrections are taken into account by the Elwert factor f_{ee}^{NR}.

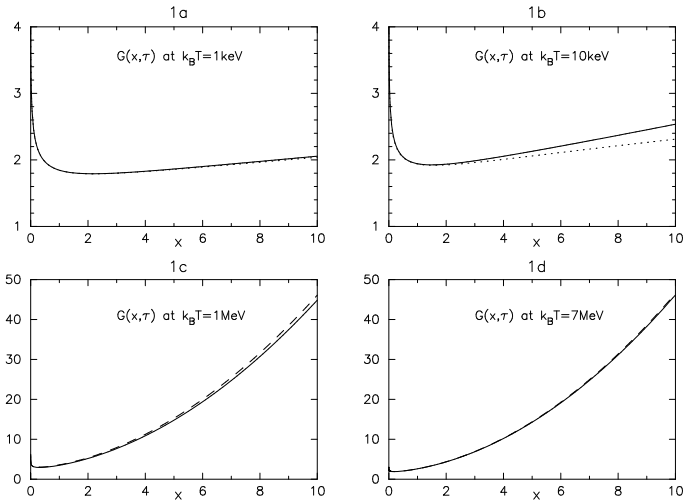

Fig. 1. Plotting of $G(x,\tau)$ as a function of x for $k_{\rm B}T = 1$ keV, 10 keV, 1 MeV, and 7 MeV. The solid curve is the full calculation of the present work. The dotted curve is the calculation in the non-relativistic approximation $G^{\rm NR}(x,\tau)$. The dashed curve is the calculation in the extreme-relativistic approximation $G^{\rm ER}(x,\tau)$.

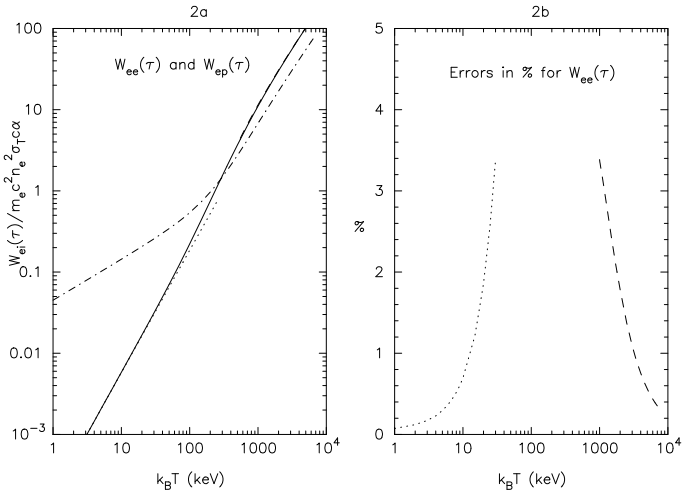

Fig. 2. Plotting of the emissivity $W_{\rm ee}(\tau)/m_{\rm e}c^2n_{\rm e}^2\sigma_{\rm T}c\alpha$ and the relative errors of the approximations. The solid curve is the full calculation of the present work. The dotted curve is the calculation in the non-relativistic approximation. The dashed curve is the calculation in the extreme-relativistic approximation. The electron-proton bremsstrahlung emissivity $W_{\rm ep}(\tau)$ is also plotted in the dash-dotted curve. In Fig. 2b, the relative errors of these approximations are plotted compared with the full calculation.

Similarly, we recall the expressions of the photon production rate and the emissivity in the extreme-relativistic (ER) approximation (Alexanian 1968) as follows:

$$P_{\rm ee}^{\rm ER}(k,\tau) = n_{\rm e}^2\sigma_{\rm T}c\alpha\frac{{\rm e}^{-x}}{x}\frac{1}{\sqrt{\tau}}G^{\rm ER}(x,\tau), \tag{19}$$

$$G^{\rm ER}(x,\tau) = \frac{3}{4\pi}\frac{1}{\sqrt{\tau}}\left\{\frac{28}{3}+2x+\frac{1}{2}x^2 +2\left(\frac{8}{3}+\frac{4}{3}x+x^2\right)(\ln(2\tau)-\gamma) -{\rm e}^x E_{\rm i}(-x)\left(\frac{8}{3}-\frac{4}{3}x+x^2\right)\right\}, \tag{20}$$

$$E_{\rm i}(-x) = -\int_x^\infty {\rm d}t\frac{{\rm e}^{-t}}{t}, \tag{21}$$

$$W_{\rm ee}^{\rm ER}(\tau) = m_{\rm e}c^2n_{\rm e}^2\sigma_{\rm T}c\alpha\tau^{3/2}\,G^{\rm ER}(\tau), \tag{22}$$

$$G^{\rm ER}(\tau) = \frac{9}{\pi\sqrt{\tau}}\left(\ln(2\tau)-\gamma+\frac{5}{4}\right), \tag{23}$$

where $E_{\rm i}(-x)$ is the exponential integral function, and $\gamma = 0.57721$ is Euler's constant.

To ascertain the extent of the approximations for the photon production rate $P_{\rm ee}(k,\tau)$, we plot $G(x,\tau)$ as a function of x at $k_{\rm B}T = 1$ keV, 10 keV, 1 MeV, and 7 MeV in Figs. 1a–d, respectively. The solid curve is the full calculation of the present work. The dotted curve represents the calculation for the non-relativistic approximation $G^{\rm NR}(x,\tau)$. The dashed curve is the calculation in the extreme-relativistic approximation $G^{\rm ER}(x,\tau)$. It can be seen from Fig. 1 that the maximum errors for the photon production rate $P_{\rm ee}(k,\tau)$ at $k_{\rm B}T = 1$ keV, 10 keV, 1 MeV, and 7 MeV are 0.9%, 9%, 6%, and 0.8%, respectively. We find that the non-relativistic approximation is accurate to within errors of 1% for $k_{\rm B}T \le 1$ keV, whereas the extreme-relativistic approximation is accurate to within errors of 1% for $k_{\rm B}T \ge 7$ MeV.

Similarly, we show the extent of the approximations for the emissivity $W_{\rm ee}(\tau)$. In Fig. 2a, we plot $W_{\rm ee}(\tau)/m_{\rm e}c^2n_{\rm e}^2\sigma_{\rm T}c\alpha$. The solid curve is the full calculation of the present work. The dotted curve is the calculation in the non-relativistic approximation. The dashed curve is the calculation in the extreme-relativistic approximation. The curves of the approximations are continuous with the curve of the full calculation at both around $k_{\rm B}T = 10$ keV and a few MeV. To compare the behavior of the electron-electron bremsstrahlung with the electron-proton bremsstrahlung, we also plot the electron-proton bremsstrahlung emissivity $W_{\rm ep}(\tau)$ calculated by Stickforth (1961) in the dash-dotted curve in Fig. 2a. One finds that $W_{\rm ee}(\tau)$ and $W_{\rm ep}(\tau)$ cross at $k_{\rm B}T = 283$ keV. This value should be compared with the reported value of $k_{\rm B}T \sim 264$ keV by Haug (1975b). For $k_{\rm B}T \ge 300$ keV, the electron-electron bremsstrahlung dominates the emissivity.

In Fig. 2b, we show the relative errors of the approximations compared with the full calculation. The dotted curve is the calculation for the non-relativistic approximation. The dashed curve is the calculation in the extreme-relativistic approximation. It can be seen from Fig. 2b that the errors in the approximations for the emissivity $W_{\rm ee}(\tau)$ are less than 1% for both $k_{\rm B}T \le 10$ keV and $k_{\rm B}T \ge 3.5$ MeV. As seen from Figs. 1 and 2, precision numerical data are now available for the photon production rate $P_{\rm ee}(k,\tau)$ and the emissivity $W_{\rm ee}(\tau)$ in the entire electron-temperature regime.

We now investigate the effect of the Coulomb corrections to the photon production rate $P_{\rm ee}(k,\tau)$. It has been known that the Coulomb corrections are important for low electron temperatures and negligible for high electron temperatures. To determine the effect of the Coulomb corrections explicitly, we define the ratio of $G(x,\tau)$ with and without Coulomb corrections as follows:

$$F_{\rm CC}(x,\tau) = \frac{G(x,\tau)}{G(x,\tau;f_{\rm ee}=1)}, \tag{24}$$

where CC denotes the Coulomb corrections. In Eq. (24), $G(x,\tau;f_{\rm ee}=1)$ corresponds to the photon production rate without Coulomb corrections, which is obtained by inserting $f_{\rm ee} = 1$ in Eq. (7). In Fig. 3, we show $F_{\rm CC}(x,\tau)$ as a function of x at $k_{\rm B}T = 1$ keV, 10 keV, 100 keV, and 300 keV. The maximum corrections at $k_{\rm B}T = 1$ keV and 10 keV are 17% and 5%,

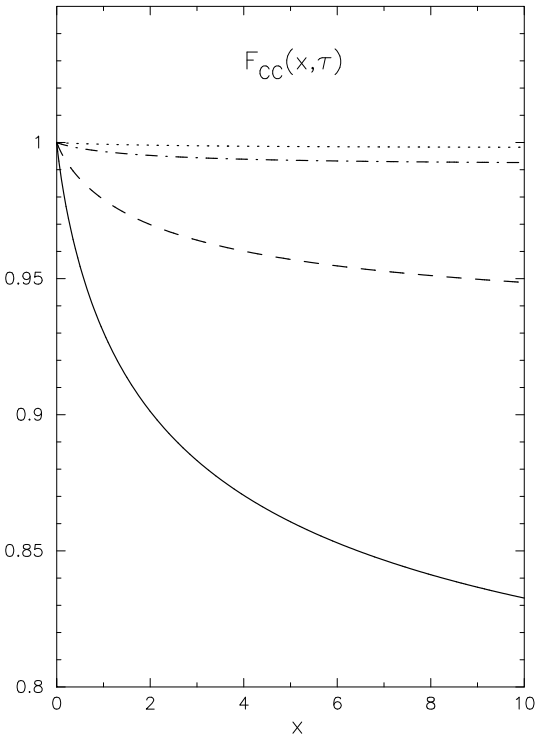

Fig. 3. Plotting of $F_{\rm CC}(x,\tau)$ as a function x. The solid curve, dashed curve, dash-dotted curve, and dotted curve are for $k_{\rm B}T = 1$ keV, 10 keV, 100 keV, and 300 keV, respectively.

respectively. The Coulomb corrections are important at low electron temperatures. On the other hand, the maximum corrections at $k_{\rm B}T = 100$ keV and 300 keV are 0.7% and 0.2%, respectively. Therefore, the Coulomb corrections can be safely neglected at $k_{\rm B}T \geq 300$ keV for the present purposes.

For the study in this section, we classify the electron temperature region for the photon production rate $P_{\rm ee}(k,\tau)$ and the emissivity $W_{\rm ee}(\tau)$ into four regions:

$$\begin{cases} k_{\rm B}T \leq 1\ {\rm keV} & \cdots & \text{region I} \\ 1\ {\rm keV} \leq k_{\rm B}T \leq 300\ {\rm keV} & \cdots & \text{region II} \\ 300\ {\rm keV} \leq k_{\rm B}T \leq 7\ {\rm MeV} & \cdots & \text{region III} \\ k_{\rm B}T \geq 7\ {\rm MeV} & \cdots & \text{region IV.} \end{cases} \tag{25}$$

In region I, the non-relativistic approximation with Coulomb corrections is sufficiently accurate within 1% errors. The full relativistic calculation with Coulomb corrections is necessary in region II. In region III, the full relativistic calculation is necessary, however, the Coulomb corrections are negligible. In region IV, the extreme-relativistic approximation is sufficiently accurate within 1% errors. In the next section, we show accurate analytic fitting formulae for the photon production rate $P_{\rm ee}(k,\tau)$ and the emissivity $W_{\rm ee}(\tau)$ in each electron temperature region defined here.

3. Analytic fitting formulae

Equations (6) and (10) provide useful tool for the data analysis of the radiation processes in active galactic nuclei, gamma-ray bursters, and compact binary sources, where electron energies may exceed 100 keV. However, the calculation of the five-dimensional integral in Eq. (7) is extremely time-consuming and therefore not practical for the analysis of the observational data. In this section, we present analytic fitting formulae for the electron-electron thermal bremsstrahlung emissivity. Stepney & Guilbert (1983) presented analytic fitting formulae for the temperature range 50 keV $\leq k_{\rm B}T \leq$ 1 MeV, which have an overall accuracy that is higher than 5% compared with the numerical integration of Eq. (7). Therefore, one task of this paper is to obtain analytic fitting formulae both of higher accuracy and a wider range of electron temperature to be useful in analyzing the precision observational data at present and also in the future. As described in the previous section, we determine the analytic fitting formulae for the photon production rate $P_{\rm ee}(k,\tau)$ and the emissivity $W_{\rm ee}(\tau)$ in region I ~ region IV separately.

3.1. Region I ($k_{\rm B}T \leq 1$ keV)

The analytic fitting formula was obtained by Itoh et al. (2002a, which we refer to IKN hereafter) for the electron-electron bremsstrahlung Gaunt factor in the non-relativistic approximation. The fitting range in the IKN paper is 50 eV $\leq k_{\rm B}T \leq$ 25 keV for the electron temperature and $10^{-4} \leq x \leq 10$ for the photon energy in units of the electron temperature. The analytic fitting formula for the photon production rate is given by

$$P^{\rm I}_{\rm ee}(k,\tau) = n_{\rm e}^2 \sigma_{\rm T} c \alpha \frac{{\rm e}^{-x}}{x} \frac{1}{\sqrt{\tau}} G^{\rm I}(x,\tau), \tag{26}$$

$$G^{\rm I}(x,\tau) = \sqrt{\frac{8}{3\pi}} \sum_{i=0}^{10} \sum_{j=0}^{10} a^{\rm I}_{ij} \Theta^i X^j, \tag{27}$$

$$\Theta = \frac{1}{1.35}(\log\tau + 2.65), \tag{28}$$

$$X = \frac{1}{2.5}(\log x + 1.50), \tag{29}$$

$$W^{\rm I}_{\rm ee}(\tau) = m_{\rm e}c^2 n_{\rm e}^2 \sigma_{\rm T} c \alpha \tau^{3/2} G^{\rm I}(\tau), \tag{30}$$

$$G^{\rm I}(\tau) = \sqrt{\frac{8}{3\pi}} \sum_{i=0}^{10} b^{\rm I}_i \Theta^i, \tag{31}$$

where $\tau = k_{\rm B}T/m_{\rm e}c^2$ and $x = k/\tau$. The numerical values of the coefficients $a^{\rm I}_{ij}$ and $b^{\rm I}_i$ are given in the IKN paper, but we include the values in Tables 1 and 2 to make the present paper more self-contained. The accuracy of the fitting formulae is superior than 0.1%.

3.2. Region II (1 keV $\leq k_{\rm B}T \leq$ 300 keV)

In this temperature region, the full relativistic calculation with Coulomb corrections is necessary for the calculation of $G(x,\tau)$. We define the fitting formulae for the photon production rate as follows:

$$P^{\rm II}_{\rm ee}(k,\tau) = n_{\rm e}^2 \sigma_{\rm T} c \alpha \frac{{\rm e}^{-x}}{x} \frac{1}{\sqrt{\tau}} G^{\rm II}_{\rm PW}(x,\tau) F^{\rm II}_{\rm CC}(x,\tau), \tag{32}$$

where $G^{\rm II}_{\rm PW}(x,\tau)$ is the fitting function for the plane-wave (PW) contribution $G(x,\tau;f_{\rm ee}=1)$. The fitting formulae are given as follows:

$$G^{\rm II}_{\rm PW}(x,\tau) = \sum_{i=0}^{2} A^{\rm II}_i(\tau) x^i - {\rm e}^x E_{\rm i}(-x) \sum_{i=0}^{1} B^{\rm II}_i(\tau) x^i, \tag{33}$$

$$A^{\rm II}_i(\tau) = \sum_{j=0}^{8} a^{\rm II}_{ij} \tau^{j/8}, \tag{34}$$

$$B^{\rm II}_i(\tau) = \sum_{j=0}^{8} b^{\rm II}_{ij} \tau^{j/8}, \tag{35}$$

where $E_{\rm i}(-x)$ is the exponential integral function defined by Eq. (21). The numerical values of the coefficients $a^{\rm II}_{ij}$ and $b^{\rm II}_{ij}$ are

Table 1. Coefficients $a_{ik}^{\rm I}$ (taken from Itoh et al. 2002a).

	$k=0$	$k=1$	$k=2$	$k=3$	$k=4$	$k=5$
$i=0$	3.15847E+0	−2.52430E+0	4.04877E−1	6.13466E−1	6.28867E−1	3.29441E−1
$i=1$	2.46819E−2	1.03924E−1	1.98935E−1	2.18843E−1	1.20482E−1	−4.82390E−2
$i=2$	−2.11118E−2	−8.53821E−2	−1.52444E−1	−1.45660E−1	−4.63705E−2	8.16592E−2
$i=3$	1.24009E−2	4.73623E−2	7.51656E−2	5.07201E−2	−2.25247E−2	−8.17151E−2
$i=4$	−5.41633E−3	−1.91406E−2	−2.58034E−2	−2.23048E−3	5.07325E−2	5.94414E−2
$i=5$	1.70070E−3	5.39773E−3	4.13361E−3	−1.14273E−2	−3.23280E−2	−2.19399E−2
$i=6$	−3.05111E−4	−7.26681E−4	4.67015E−3	1.24789E−2	−1.16976E−2	−1.13488E−2
$i=7$	−1.21721E−4	−7.47266E−4	−2.20675E−3	−2.74351E−3	−1.00402E−3	−2.38863E−3
$i=8$	1.77611E−4	8.73517E−4	−2.67582E−3	−4.57871E−3	2.96622E−2	1.89850E−2
$i=9$	−2.05480E−5	−6.92284E−5	2.95254E−5	−1.70374E−4	−5.43191E−4	2.50978E−3
$i=10$	−3.58754E−5	−1.80305E−4	1.40751E−3	2.06757E−3	−1.23098E−2	−8.81767E−3

	$k=6$	$k=7$	$k=8$	$k=9$	$k=10$
$i=0$	−1.71486E−1	−3.68685E−1	−7.59200E−2	1.60187E−1	8.37729E−2
$i=1$	−1.20811E−1	−4.46133E−4	8.88749E−2	2.50320E−2	−1.28900E−2
$i=2$	9.87296E−2	−3.24743E−2	−8.82637E−2	−7.52221E−3	1.99419E−2
$i=3$	−4.59297E−2	5.05096E−2	5.58818E−2	−9.11885E−3	−1.71348E−2
$i=4$	−2.11247E−2	−5.05387E−2	9.20453E−3	1.67321E−2	−3.47663E−3
$i=5$	1.76310E−2	2.23352E−2	−4.59817E−3	−8.24286E−3	−3.90032E−4
$i=6$	6.31446E−2	1.33830E−2	−8.54735E−2	−6.47349E−3	3.72266E−2
$i=7$	−2.28987E−3	7.79323E−3	7.98332E−3	−3.80435E−3	−4.25035E−3
$i=8$	−8.84093E−2	−2.93629E−2	1.02966E−1	1.38957E−2	−4.22093E−2
$i=9$	4.45570E−3	−2.80083E−3	−5.68093E−3	1.10618E−3	2.33625E−3
$i=10$	3.46210E−2	1.23727E−2	−4.04801E−2	−5.68689E−3	1.66733E−2

Table 2. Coefficients $b_i^{\rm I}$ (taken from Itoh et al. 2002a).

	$b_i^{\rm I}$
$i=0$	2.21564E+0
$i=1$	1.83879E−1
$i=2$	−1.33575E−1
$i=3$	5.89871E−2
$i=4$	−1.45904E−2
$i=5$	−7.10244E−4
$i=6$	2.80940E−3
$i=7$	−1.70485E−3
$i=8$	5.26075E−4
$i=9$	9.94159E−5
$i=10$	−1.06851E−4

shown in Table 3. In Eq. (32), $F_{\rm CC}^{\rm II}(x,\tau)$ is the fitting function for the Coulomb corrections $F_{\rm CC}(x,\tau)$ defined by Eq. (24). It is given by

$$F_{\rm CC}^{\rm II}(x,\tau) = 1+\sum_{i=2}^{6} C_i^{\rm II}(\tau)x^{i/8}, \tag{36}$$

$$C_i^{\rm II}(\tau) = \sum_{j=0}^{6} c_{ij}^{\rm II}\tau^{j/6}. \tag{37}$$

The numerical values of the coefficients $c_{ij}^{\rm II}$ are shown in Table 4. The fitting region for $G_{\rm PW}^{\rm II}(x,\tau)$ and $F_{\rm CC}^{\rm II}(x,\tau)$ is given by 1 keV $\le k_{\rm B}T \le$ 300 keV and $10^{-4} \le x \le 10$. In Figs. 4a and b, we show the relative errors of $G_{\rm PW}^{\rm II}(x,\tau)$ and $F_{\rm CC}^{\rm II}(x,\tau)$ compared with the numerical values, respectively. The solid curve, dashed curve, dash-dotted curve, and dotted curve represent $k_{\rm B}T$ = 1 keV, 10 keV, 100 keV, and 300 keV, respectively. One can see from Fig. 4 that the maximum errors are 0.5% and 0.2% for $G_{\rm PW}^{\rm II}(x,\tau)$ and $F_{\rm CC}^{\rm II}(x,\tau)$, respectively. The errors in the photon production rate $P_{\rm ee}^{\rm II}(k,\tau)$ are found to be less than 0.5%.

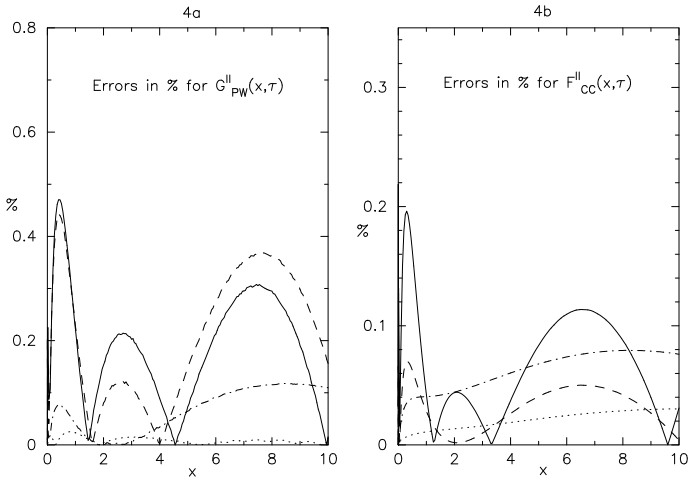

Fig. 4. Plotting of errors for the analytic fitting functions $G_{\rm PW}^{\rm II}(x,\tau)$ and $F_{\rm CC}^{\rm II}(x,\tau)$. The solid curve, dashed curve, dash-dotted curve, and dotted curve are for $k_{\rm B}T$ = 1 keV, 10 keV, 100 keV, and 300 keV, respectively.

In a similar way, the fitting function for the emissivity $W_{\rm ee}^{\rm II}(\tau)$ is given as follows:

$$W_{\rm ee}^{\rm II}(\tau) = m_{\rm e}c^2 n_{\rm e}^2 \sigma_{\rm T} c\alpha\tau^{3/2}\, G^{\rm II}(\tau), \tag{38}$$

$$\begin{aligned} G^{\rm II}(\tau) &= A_0^{\rm II}(\tau)+A_1^{\rm II}(\tau)+2A_2^{\rm II}(\tau) \\ &\quad +B_0^{\rm II}(\tau)+\frac{1}{2}B_1^{\rm II}(\tau) \\ &\quad +\sum_{i=0}^{2}\sum_{j=2}^{6}\Gamma\left(i+\frac{j}{8}+1\right)A_i^{\rm II}(\tau)C_j^{\rm II}(\tau) \\ &\quad +\sum_{i=0}^{1}\sum_{j=2}^{6}\frac{\Gamma(i+\frac{j}{8}+1)}{i+\frac{j}{8}+1}B_i^{\rm II}(\tau)C_j^{\rm II}(\tau), \end{aligned} \tag{39}$$

where $\Gamma(i+j/8+1)$ is the Γ-function. The fitting region is 1 keV $\le k_{\rm B}T \le$ 300 keV. We find that the errors are less than 0.2%.

Table 3. Coefficients $a_{ij}^{\rm II}$ and $b_{ij}^{\rm II}$.

	$a_{0j}^{\rm II}$	$a_{1j}^{\rm II}$	$a_{2j}^{\rm II}$	$b_{0j}^{\rm II}$	$b_{1j}^{\rm II}$
$j=0$	−3.7369800E+1	−9.3647000E+0	9.2170000E−1	−1.1628100E+1	−8.6991000E+0
$j=1$	3.8036590E+2	9.5918600E+1	−1.3498800E+1	1.2560660E+2	6.3383000E+1
$j=2$	−1.4898014E+3	−3.9701720E+2	7.6453900E+1	−5.3274890E+2	−1.2889390E+2
$j=3$	2.8614150E+3	8.4293760E+2	−2.1783010E+2	1.1423873E+3	−1.3503120E+2
$j=4$	−2.3263704E+3	−9.0730760E+2	3.2097530E+2	−1.1568545E+3	9.7758380E+2
$j=5$	−6.9161180E+2	3.0688020E+2	−1.8806670E+2	7.5010200E+1	−1.6499529E+3
$j=6$	2.8537893E+3	2.9129830E+2	−8.2416100E+1	9.9681140E+2	1.2586812E+3
$j=7$	−2.0407952E+3	−2.9902530E+2	1.6371910E+2	−8.8818950E+2	−4.0474610E+2
$j=8$	4.9259810E+2	7.6346100E+1	−6.0024800E+1	2.5013860E+2	2.7335400E+1

Table 4. Coefficients $c_{ij}^{\rm II}$.

	$c_{2j}^{\rm II}$	$c_{3j}^{\rm II}$	$c_{4j}^{\rm II}$	$c_{5j}^{\rm II}$	$c_{6j}^{\rm II}$
$j=0$	−5.7752000E+0	3.0558600E+1	−5.4327200E+1	3.6262500E+1	−8.4082000E+0
$j=1$	4.6209700E+1	−2.4821770E+2	4.5096760E+2	−3.1009720E+2	7.4792500E+1
$j=2$	−1.6072800E+2	8.7419640E+2	−1.6165987E+3	1.1380531E+3	−2.8295400E+2
$j=3$	3.0500700E+2	−1.6769028E+3	3.1481061E+3	−2.2608347E+3	5.7639300E+2
$j=4$	−3.2954200E+2	1.8288677E+3	−3.4783930E+3	2.5419361E+3	−6.6193900E+2
$j=5$	1.9107700E+2	−1.0689366E+3	2.0556693E+3	−1.5252058E+3	4.0429300E+2
$j=6$	−4.6271800E+1	2.6056560E+2	−5.0567890E+2	3.8008520E+2	−1.0223300E+2

Table 5. Coefficients $a_{ij}^{\rm III}$ and $b_{ij}^{\rm III}$.

	$a_{0j}^{\rm III}$	$a_{1j}^{\rm III}$	$a_{2j}^{\rm III}$	$b_{0j}^{\rm III}$	$b_{1j}^{\rm III}$
$j=0$	5.2163300E+1	4.9713900E+1	6.4751200E+1	−8.5862000E+0	3.7643220E+2
$j=1$	−2.5703130E+2	−1.8977460E+2	−2.1389560E+2	3.4134800E+1	−1.2233635E+3
$j=2$	4.4681610E+2	2.7102980E+2	1.7414320E+2	−1.1632870E+2	6.2867870E+2
$j=3$	−2.9305850E+2	−2.6978070E+2	1.3650880E+2	2.9654510E+2	2.2373946E+3
$j=4$	0.0000000E+0	4.2048120E+2	−2.7148990E+2	−3.9342070E+2	−3.8288387E+3
$j=5$	7.7047400E+1	−5.7662470E+2	8.9321000E+1	2.3754970E+2	2.1217933E+3
$j=6$	−2.3871800E+1	4.3277900E+2	5.8258400E+1	−3.0600000E+1	−5.5166700E+1
$j=7$	0.0000000E+0	−1.6053650E+2	−4.6080700E+1	−2.7617000E+1	−3.4943210E+2
$j=8$	1.9970000E−1	2.3392500E+1	8.7301000E+0	8.8453000E+0	9.2205900E+1

3.3. Region III (300 keV ≤ $k_{\rm B}T$ ≤ 7 MeV)

In this temperature region, the full relativistic calculation is necessary for the calculation of $G(x,\tau)$, although the Coulomb corrections are negligible. We define the fitting formula for the photon production rate as follows:

$$P_{\rm ee}^{\rm III}(k,\tau) = n_{\rm e}^2\sigma_{\rm T}c\alpha\frac{{\rm e}^{-x}}{x}\frac{1}{\sqrt{\tau}}G_{\rm PW}^{\rm III}(x,\tau), \quad (40)$$

$$G_{\rm PW}^{\rm III}(x,\tau) = \sum_{i=0}^{2}A_i^{\rm III}(\tau)x^i - {\rm e}^x E_{\rm i}(-x)\sum_{i=0}^{1}B_i^{\rm III}(\tau)x^i, \quad (41)$$

$$A_i^{\rm III}(\tau) = \sum_{j=0}^{8}a_{ij}^{\rm III}\tau^{j/8}, \quad (42)$$

$$B_i^{\rm III}(\tau) = \sum_{j=0}^{8}b_{ij}^{\rm III}\tau^{j/8}, \quad (43)$$

where $E_{\rm i}(-x)$ is the exponential integral function defined by Eq. (21). The numerical values of the coefficients $a_{ij}^{\rm III}$ and $b_{ij}^{\rm III}$ are shown in Table 5. The fitting region for $G_{\rm PW}^{\rm III}(x,\tau)$ is 300 keV ≤ $k_{\rm B}T$ ≤ 7 MeV and 10^{-4} ≤ x ≤ 10. In Fig. 5, we show the relative errors of $G_{\rm PW}^{\rm III}(x,\tau)$ compared with the numerical values as a function x. The solid curve, dashed curve, and dotted curve are for $k_{\rm B}T$ = 300 keV, 1 MeV, and 7 MeV, respectively. One can see from Fig. 5 that the maximum error in the analytic fitting function is 0.2%. In Fig. 5, we also plot the relative error for $G^{\rm ER}(x,\tau)$ at $k_{\rm B}T$ = 7 MeV compared with the full caluclation in dash-dotted curve. The maximum error in the extreme-relativistic approximation is 0.8% as described in the previous section.

Similarly, the fitting formula for the the emissivity $W_{\rm ee}^{\rm III}(\tau)$ is given as follows:

$$W_{\rm ee}^{\rm III}(\tau) = m_{\rm e}c^2 n_{\rm e}^2\sigma_{\rm T}c\alpha\tau^{3/2}G^{\rm III}(\tau), \quad (44)$$

$$G^{\rm III}(\tau) = A_0^{\rm III}(\tau) + A_1^{\rm III}(\tau) + 2A_2^{\rm III}(\tau) + B_0^{\rm III}(\tau) + \frac{1}{2}B_1^{\rm III}(\tau). \quad (45)$$

The fitting region is 300 keV ≤ $k_{\rm B}T$ ≤ 7 MeV. We find that the error is less than 0.1%.

3.4. Region IV ($k_{\rm B}T$ ≥ 7 MeV)

In this temperature region, the extreme-relativistic approximation (Alexanian 1968) is sufficiently accurate to within the 1% errors. The explicit forms of the photon production rate and the emissivity have already been shown in the previous section.

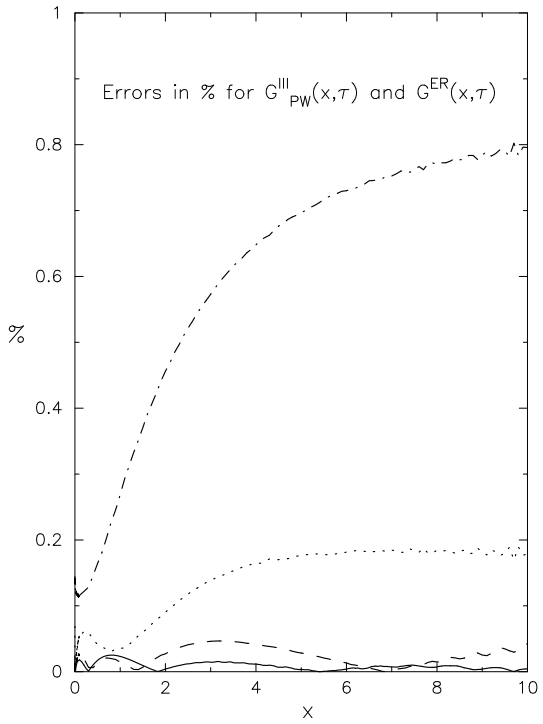

Fig. 5. Plotting of the errors for the analytic fitting function $G^{\rm III}_{\rm PW}(x,\tau)$ and the extreme-relativistic approximation $G^{\rm ER}(x,\tau)$. The solid curve, dashed curve, and dotted curve are for $G^{\rm III}_{\rm PW}(x,\tau)$ at $k_{\rm B}T = 300$ keV, 1 MeV, and 7 MeV, respectively. The dash-dotted curve is for $G^{\rm ER}(x,\tau)$ at $k_{\rm B}T = 7$ MeV.

They are as follows:

$$P^{\rm IV}_{\rm ee}(k,\tau) = n_{\rm e}^2\sigma_{\rm T}c\alpha\frac{{\rm e}^{-x}}{x}\frac{1}{\sqrt{\tau}}\,G^{\rm ER}(x,\tau), \quad (46)$$

$$W^{\rm IV}_{\rm ee}(\tau) = m_{\rm e}c^2 n_{\rm e}^2\sigma_{\rm T}c\alpha\tau^{3/2}\,G^{\rm ER}(\tau), \quad (47)$$

where $G^{\rm ER}(x,\tau)$ and $G^{\rm ER}(\tau)$ are Eqs. (20) and (23), respectively.

4. Concluding remarks

We have studied the relativistic electron-electron thermal bremsstrahlung based upon the approaches given by Haug (1975a,b), and Stepney & Guilbert (1983). The photon production rate $P_{\rm ee}(k,\tau)$ and the emissivity $W_{\rm ee}(\tau)$ were calculated for the electron temperature 1 keV $\le k_{\rm B}T \le$ 7 MeV and for $10^{-4} \le x \le 10$, where x is the photon energy in units of the electron temperature. We have calculated the analytic fitting formulae for the numerical data of both the photon production rate and the emissivity. The obtained analytic fitting formulae have reproduced the numerical integration of Eq. (7) to within 0.5% errors for 1 keV $\le k_{\rm B}T \le$ 7 MeV. We have also found that the non-relativistic approximation can be used within its 1% errors for $k_{\rm B}T \le 1$ keV, whereas the extreme-relativistic approximation can be used within its 1% errors for $k_{\rm B}T \ge 7$ MeV. Combining the existing analytic expressions for the non-relativistic approximations and the extreme-relativistic approximations, we have obtained analytic fitting formulae for $P_{\rm ee}(k,\tau)$ and $W_{\rm ee}(\tau)$ in the entire electron temperature regime. We summarize the expressions of the analytic fitting formulae for the photon production rate and the emissivity as follows:

$$P^{\rm fit}_{\rm ee}(x,\tau) = 1.455\times10^{-16}[n_{\rm e}({\rm cm}^{-3})]^2 \times\frac{{\rm e}^{-x}}{x}\frac{1}{\sqrt{\tau}}\,G^{\rm fit}(x,\tau) \quad {\rm cm}^{-3}\ {\rm s}^{-1}, \quad (48)$$

$$G^{\rm fit}(x,\tau) = \begin{cases} G^{\rm I}(x,\tau) & \text{for region I} \\ G^{\rm II}_{\rm PW}(x,\tau)F^{\rm II}_{\rm CC}(x,\tau) & \text{for region II} \\ G^{\rm III}_{\rm PW}(x,\tau) & \text{for region III} \\ G^{\rm ER}(x,\tau) & \text{for region IV.} \end{cases} \quad (49)$$

$$W^{\rm fit}_{\rm ee}(\tau) = 1.192\times10^{-22}[n_{\rm e}({\rm cm}^{-3})]^2 \times\tau^{3/2}\,G^{\rm fit}(\tau) \quad {\rm erg\,cm}^{-3}\ {\rm s}^{-1}, \quad (50)$$

$$G^{\rm fit}(\tau) = \begin{cases} G^{\rm I}(\tau) & \text{for region I} \\ G^{\rm II}(\tau) & \text{for region II} \\ G^{\rm III}(\tau) & \text{for region III} \\ G^{\rm ER}(\tau) & \text{for region IV.} \end{cases} \quad (51)$$

In Eqs. (49) and (51) the regions I–IV are defined by Eq. (25). The present analytic fitting formulae will be useful for the analysis of the precision observational data acquired by the *Chandra X-Ray Observatory*, the *XMM-Newton X-ray Observatory*, the *Suzaku X-ray Observatory*, and the next generation X-ray and gamma-ray observatories for the electron energies from non-relativistic regime to mildly-relativistic regime. Assuming the thermal plasma, the present formulae will be also applicable to relativistic regime. Finally, the subroutines of all the fitting formulae will de downloadable from our website[1].

Acknowledgements. We wish to thank our referee for many useful suggestions. We wish to thank Prof. Y. Oyanagi for allowing us to use the least squares fitting program SALS.

References

Alexanian, M. 1968, Phys. Rev., 165, 253
Allen, S. W., Ettori, S., & Fabian, A. C. 2001, MNRAS, 324, 877
Dermer, C. D. 1986, ApJ, 307, 47
Elwert, G. 1939, Ann. Phys., 34, 178
Haug, E. 1975a, Z. Naturforsch., 30a, 1099
Haug, E. 1975b, Z. Naturforsch., 30a, 1546
Itoh, N., Sakamoto, T., Kusano, S., Nozawa, S., & Kohyama, Y. 2000, ApJS, 128, 125
Itoh, N., Kawana, Y., & Nozawa, S. 2002a, Il Nuovo Cimento, 117B, 359
Itoh, N., Sakamoto, T., Kusano, S., Kawana, Y., & Nozawa, S. 2002b, A&A, 382, 722
Maxon, M. S. 1972, Phys. Rev. A, 5, 1630
Maxon, M. S., & Corman, E. G. 1967, Phys. Rev., 163, 156
Nozawa, S., Itoh, N., & Kohyama, Y. 1998, ApJ, 507, 530
Sato, K., Yamasaki, N. Y., Ishida, M., et al. 2007, PASJ, 59, 299
Schmidt, R. W., Allen, S. W., & Fabian, A. C. 2001, MNRAS, 327, 1057
Stepney, S., & Guilbert, P. W. 1983, MNRAS, 204, 1269
Stickforth, J. 1961, Z. Phys., 164, 1
Svensson, R. 1982, ApJ, 258, 335

[1] http://www.ph.sophia.ac.jp/~itoh-ken/english/research.htm